Biochemical and Biophysical Research Communications 435 (2013) 657–663

Contents lists available at SciVerse ScienceDirect

Biochemical and Biophysical Research Communications

journal homepage: www.elsevier.com/locate/ybbrc

Novel tamoxifen derivative Ridaifen-B induces Bcl-2 independent autophagy without estrogen receptor involvement

Yukitoshi Nagahara [a,*], Midori Takeyoshi [a], Seiya Sakemoto [a], Isamu Shiina [b], Kenya Nakata [b], Keiko Fujimori [b], Yanwen Wang [b], Eri Umeda [b], Chihiro Watanabe [b], Shoko Uetake [b], Takao Yamori [c], Shingo Dan [c], Yoji Yoshimi [d], Takahisa Shinomiya [d], Masahiko Ikekita [d]

[a] Department of Biotechnology, College of Science and Engineering, Tokyo Denki University, Hatoyama, Hiki-gun, Saitama 350-0394, Japan
[b] Department of Applied Chemistry, Faculty of Science, Tokyo University of Science, Kagurazaka, Shinjuku-ku, Tokyo 162-8601, Japan
[c] Division of Molecular Pharmacology, Cancer Chemotherapy Center, Japanese Foundation for Cancer Research, Ariake, Koto-ku, Tokyo 135-8550, Japan
[d] Department of Applied Biological Science, Faculty of Science and Technology, Tokyo University of Science, 2641 Yamazaki, Noda, Chiba 278-8510, Japan

ARTICLE INFO

Article history:
Received 8 May 2013
Available online 18 May 2013

Keywords:
Ridaifen-B
Autophagy
LC3
Bcl-2
Beclin 1

ABSTRACT

Autophagy is a self-proteolysis process in eukaryotic cells that results in the sequestering of intracellular proteins and organelles in autophagosomes. Activation of autophagy progress continued growth of some tumors, instead extensive autophagy induces cell death. In a previous study, we synthesized a novel tamoxifen derivative, Ridaifen (RID)-B. RID-B induced mitochondria-involved apoptosis even in estrogen receptor (ER)-negative cells. Since tamoxifen induces autophagy other than apoptosis, we treated ER-negative Jurkat cells with RID-B in the present study. RID-B treatment induced apoptosis and LC3 and lysosome colocalization, which results in the formation of autolysosomes. Western blotting revealed that LC3 was converted to LC3-I to LC3-II with RID-B treatment, suggesting that RID-B induced autophagy without ER involvement. Moreover, overexpression of the anti-apoptotic protein Bcl-2 suppressed the RID-B-induced cell death, but not the induction of autophagy. These results presumed that RID-B-induced autophagy is independent of Bcl-2, making RID-B-induced autophagy different from RID-B-induced apoptosis. Since Beclin 1 level is unchanged during RID-B treatment, RID-B induced autophagy pathway is Bcl-2/Beclin1 independent noncanonical pathway.

1. Introduction

Autophagy is an evolutionarily conserved self-proteolysis process in eukaryotic cells that functions to provide an alternative source of energy and thus enable cells to survive under cellular stress conditions such as nutrient-deficient environments and the accumulation of damaged proteins and organelles [1–3]. Autophagy involves the sequestration of cellular components within a membrane, the so-called 'autophagosome'. Autophagosomes then fuse with endosomes or directly with lysosomes to form autolysosomes, resulting in the degradation of their components by hydrolytic enzymes.

The process of autophagy is controlled by a group of autophagy-related genes (Atg) [4]. First, the formation of the phagophore is related to phosphatidylinositol kinase class III Vps34 and Beclin 1 (mammalian ortholog of Atg6) [5]. Next, elongation of the phagophore membrane and formation of the autophagosome are accomplished by two ubiquitin-like conjugation systems, Atg5-Atg12 and LC3 (mammalian ortholog of Atg8) [6]. This Beclin 1 and Vps34 dependent autophagy is so-called conventional autophagy. A serine/threonine protein kinase, mammalian target of rapamycin (mTOR) plays an important role in the control of conventional autophagy pathway upstream of Beclin 1 and Vps34 [7]. Under starvation conditions, mTOR become inactivated and precede autophagy [8]. Moreover, the anti-apoptotic protein Bcl-2 binds to Beclin 1 and inhibits this conventional autophagy process [9,10], with resulting cross-talk among cell growth, proliferation, survival and death.

Activation of the autophagy progress induces the growth of some tumors, serving to both reduce oxidative stress and sustain cell metabolism [11]. However, extensive autophagy sometimes kills cells resulting in the accumulation of autophagosomes in dying cells [12]. This dual role of autophagy – cell survival and cell death – is complex, and there are many chemicals that induce autophagy for cell survival or cell death [13,14]. For example, the breast cancer drug tamoxifen is a strong inducer of apoptosis and autophagy [15,16].

Ridaifen (RID)-B is a novel tamoxifen derivative. In a previous study, we observed that RID-B had more potent cancer cell-damag-

* Corresponding author. Fax: +81 49 296 5162.
E-mail address: yuki@mail.dendai.ac.jp (Y. Nagahara).

0006-291X/$ - see front matter © 2013 Elsevier Inc. All rights reserved.
http://dx.doi.org/10.1016/j.bbrc.2013.05.040

ing activity than tamoxifen [17]. RID-B fragmented Jurkat cells' DNA and activated caspases, suggesting that the RID-B-induced apoptosis pathway is estrogen receptor (ER)-independent. We also estimated the mitochondrial involvement during RID-B-induced apoptosis: RID-B significantly reduced the mitochondrial membrane potential, and the overexpression of Bcl-2 inhibited the RID-B-induced apoptosis phenomena. These results suggested that the induction of apoptosis by RID-B is dependent on mitochondrial perturbation without ER involvement. However, little is known about the involvement of autophagy by RID-B. In the present study, we found that RID-B induced autophagy in the ER-negative human lymphoma Jurkat cell line. The RID-B-induced autophagy was independent of Bcl-2 and Beclin 1 activity, suggesting that the RID-B-induced autophagy pathway is different from the conventional autophagy pathway.

2. Materials and methods

2.1. Cells

The human lymphoid helper T-cell line, Jurkat, stably transfected with a human Bcl-2 expression plasmid (Bcl-2) or neomycin resistance plasmid (neo), was provided by Dr. T. Miyashita of Kitasato University (Sagamihara, Japan). Human hepatoma HepG2 cells were supplied by the Cell Resource Center for Biomedical Research, Institute of Development, Aging and Cancer Tohoku University (Sendai, Japan).

2.2. Media and cell cultures

The Jurkat cells were cultured in RPMI-1640 medium supplemented with 10% fetal bovine serum (FBS) and 75 mg/L kanamycin sulfate, and maintained at 37 °C in a humidified chamber under an atmosphere of 95% air and 5% CO_2. The HepG2 cells were maintained at 37 °C with 5% CO_2 in DMEM supplemented with streptomycin and 10% (v/v) FBS.

2.3. Chemicals and antibodies

Tamoxifen and RID-B (Fig. 1A) were chemically synthesized in our laboratory based on the methods described by Shiina et al. [18,19]. Anti-LC3B and β-actin antibodies were purchased from Cell Signaling Technologies (Danvers, MA). Anti-Bcl-2 and Caspase-3 antibodies were purchased from Santa Cruz Biotechnologies (Santa Cruz, CA). Anti-Beclin 1 antibody was purchased from BD Bioscience (San Jose, CA).

2.4. MTT assay

The cells were incubated in 96-well plates at 37 °C with RID-B for 23 h. Then, 10 μL of 5 mg/mL 3-(4,5-dimethylthiazol-2-yl)-2,5-diphenyl tetrazolium bromide (MTT; Wako, Osaka, Japan) was added to each well and the plates were incubated at 37 °C for 1 h. The media were discarded, and 100 μL of dimethyl sulfoxide was added to dissolve MTT formazan. The absorbance of each well was measured using a microplate reader (Corona Electrics, Hitachinaka, Japan) at 570 nm.

2.5. Assessment of sub-G1 cells and cell cycle

Cells (1×10^6) were washed with phosphate buffered saline (PBS) and suspended in permeabilizing buffer (0.1% Triton-X 100 in PBS). Thereafter, the cells were washed with PBS, resuspended in PBS containing 0.5 mg/mL RNase A and 2 μg/mL propidium iodide (PI), and analyzed by flow cytometry (FACS Calibur, Beckton Dickinson, Mountain View, CA). Data were analyzed using Cell Quest (Beckton Dickinson).

2.6. Detection of caspase activities

The activation of caspases was determined by measuring the hydrolyzing activities of caspase-3 substrate, acetyl-DEVD-4-methyl-coumaryl-7-amide (Ac-DEVD-MCA; Alexis, San Diego, CA). Cells (1×10^7) were lysed in RIPA buffer (25 mM Tris, pH 7.4, 150 mM KCl, 5 mM EDTA, 1% Nonidet P-40, 0.5% sodium deoxycholate, 0.1% SDS), and cell extracts were obtained by centrifugation at 13,000*g* for 5 min at 4 °C. The protein concentration was determined using the BCA protein assay. Cell extracts were preincubated in 250 μL of caspase buffer (50 mM HEPES, pH 7.4, 100 mM NaCl, 1 mM EDTA, 0.1% Chaps, 10% sucrose, 5 mM dithiothreitol) containing 80 μM substrate and Ac-DEVD-MCA and incubated at 37 °C for 1 h. The mixture was centrifuged, and the release of 7-amino-4-methyl-coumarin in the supernatant was measured using the spectrofluorometer (Corona Electrics) at excitation and emission wavelengths of 365 nm and 450 nm, respectively.

2.7. Confocal microscopic analysis of colocalization of LC3 and lysosomes

Cells were labeled by incubation with Lysotracker Red (Takara Bio, Shiga, Japan), for 90 min at 37 °C. Thereafter, cells were fixed with 4% *p*-formaldehyde for 20 min and permeabilized with 1% CHAPS buffer (150 mM NaCl, 10 mM HEPES, 1.0% CHAPS) at room temperature for 10 min. Thereafter, cells were incubated with anti-LC3B monoclonal antibody overnight at 4 °C, washed with PBS, and incubated for another 60 min with Alexa Fluor 488-conjugated anti-rabbit IgG antibody. Then, cell nuclei were stained by DAPI (Wako). Samples were examined under a confocal microscope system (FV10i-DOC, Olympus, Tokyo).

2.8. Western blotting

Cells were washed with PBS and placed on ice for 20 min in lysis buffer (50 mM HEPES–NaOH, 10% glycerol, 150 mM NaCl, 1% Triton X-100, 1 mM EGTA, 1.5 mM $MgCl_2$, 1% proteinase inhibitor cocktail [Sigma, St. Louis, MO], pH 7.5, 0.1 mM sodium orthovanadate). Cell lysates were centrifuged at 4 °C for 15 min at 13,000*g*. Protein concentrations of the supernatant were determined using the BCA protein assay (Thermo Scientific, Waltham, MA). Cell lysates (30 μg) were mixed in the same volume of sodium dodecyl sulfate (SDS) sample buffer (4% SDS, 125 mM Tris, pH 6.8, 10% glycerol, 0.02 mg/mL bromophenol blue, 10% 2-mercaptoethanol) and heated at 100 °C for 3 min. Proteins were separated by 10% polyacrylamide gel SDS-electrophoresis and electrically transferred to a PVDF membrane (Bio-Rad Laboratories, Hercules, CA). After the membrane was blocked with the use of 3% skimmed milk, Caspase-3, LC3, Beclin 1, Bcl-2, and β-actin were immunodetected using specific antibodies. Thereafter, horseradish peroxidase-conjugated anti-rabbit IgG was applied as the second antibody, and positive bands were detected by enhanced chemiluminescence (Thermo Scientific). Visualization was done with an Image Quant LAS-4000 digital imaging system (GE Healthcare, Buckinghamshire, UK).

3. Results

3.1. RID-B induces apoptosis in ER-negative Jurkat cells

In our previous study, we synthesized a novel tamoxifen derivative, RID-B, and treated ER-negative human T-cell lymphoma Jur-

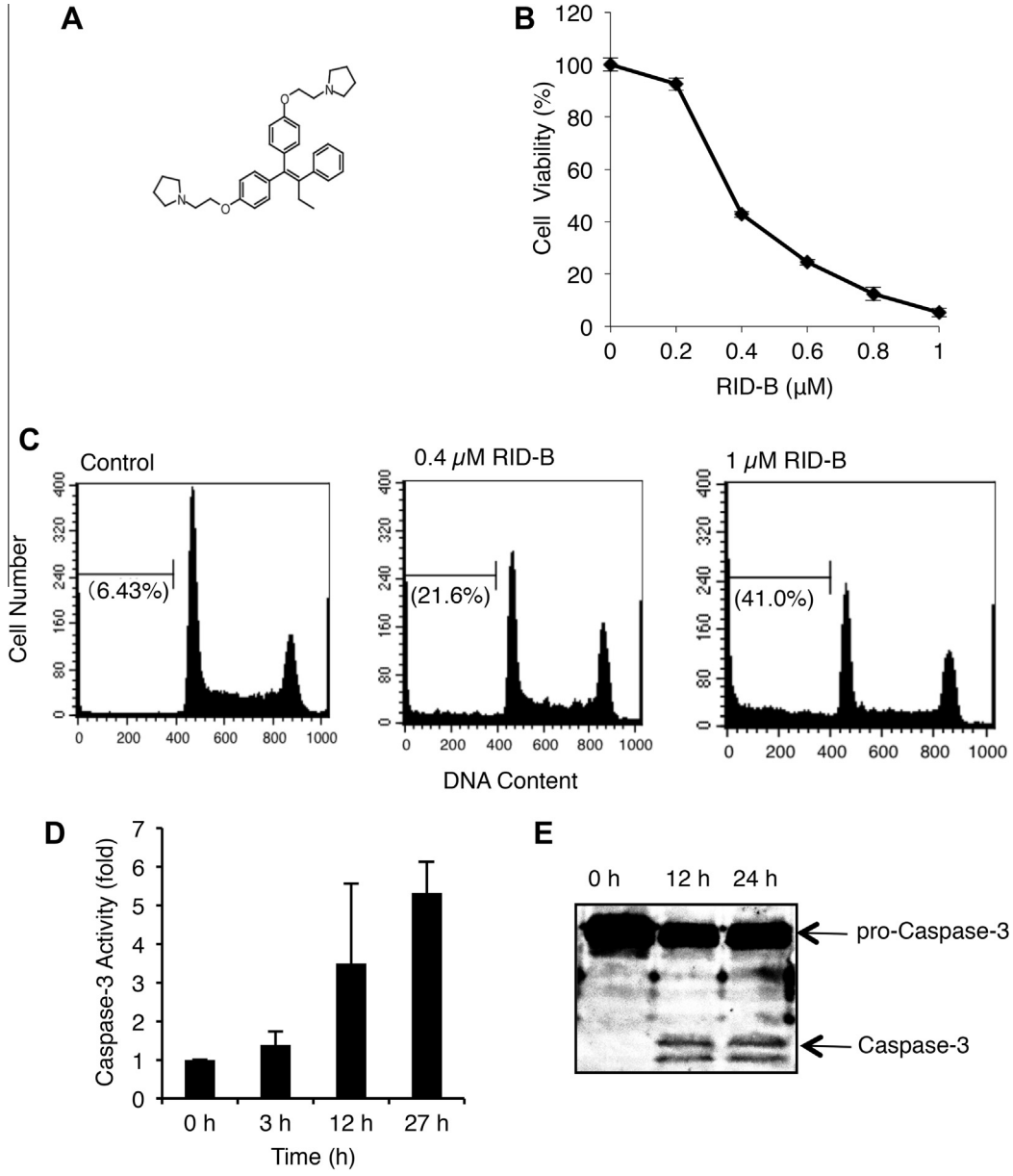

Fig. 1. RID-B induced apoptosis in ER-negative cells. (A) Chemical structure of RID-B. (B) Jurkat cells were incubated with indicated doses of RID-B for 24 h. Cell proliferation was estimated by MTT assay. The data are presented as a comparison to the nonadditive control cells. Each bar denotes the std. dev. (n = 3). (C) Jurkat cells were incubated with indicated doses of RID-B for 24 h and assayed flow cytometrically as described in Section 2. Data are representative of three independent experiments. Parentheses indicate the percentages of sub-G1 phase. (D) Jurkat cells were incubated with 0.4 μM RID-B for the indicated times. The cells were lysed and subjected to a caspase-3 assay as described in Section 2. The results are presented as a comparison to the 0-h treatment. Each bar = std. dev. (n = 3). (E) Jurkat cells were incubated with 0.4 μM RID-B for the indicated times. The cells were lysed and Caspase-3 was detected by Western blotting.

kat cells with it [17]. Four-hour treatment with RID-B damaged the Jurkat cells in a dose-dependent manner. The IC_{50} rate was 4 μM. Treatment with an antitumor drug is usually for a longer period than that used in our previous study (4-h). Thus, in the present study, first we examined the long-term effect of RID-B on Jurkat cells. As shown in Fig. 1B, 24-h treatment with RID-B injured Jurkat cells in a dose-dependent manner, similar to the previous results obtained with short-term (4-h) RID-B treatment. The IC_{50} rate was about 0.4 μM. We also evaluated RID-B-mediated cell death in the long-term treatment. The flow cytometric analysis revealed that RID-B treatment significantly increased the sub-G1 phase of DNA contents in a dose-dependent manner, indicating that DNA fragmentation is induced by RID-B (Fig. 1C). In addition, the 0.4 μM RID-B treatment activated Caspase-3 in a time-dependent manner (Fig. 1D), as well as cleaved pro-Caspase-3 to active Caspase-3 (Fig. 1E). These results demonstrated that long-term (24-h) treatment with a low concentration (0.4 μM) of RID-B induced apoptosis in ER-negative Jurkat cells.

3.2. RID-B induces autophagy

Tamoxifen induces autophagy in cancer cells [15,16]. We therefore hypothesized that the tamoxifen derivative RID-B would also induce autophagy. To evaluate the autophagy by RID-B, we observed the localization of LC3 in cells before and after RID-B treatment, by indirect immunofluorescence staining. During autophagy, the cytoplasmic form of LC3 (LC3-I) is processed and recruited to autophagosomes, where LC3-II is generated by site-specific prote-

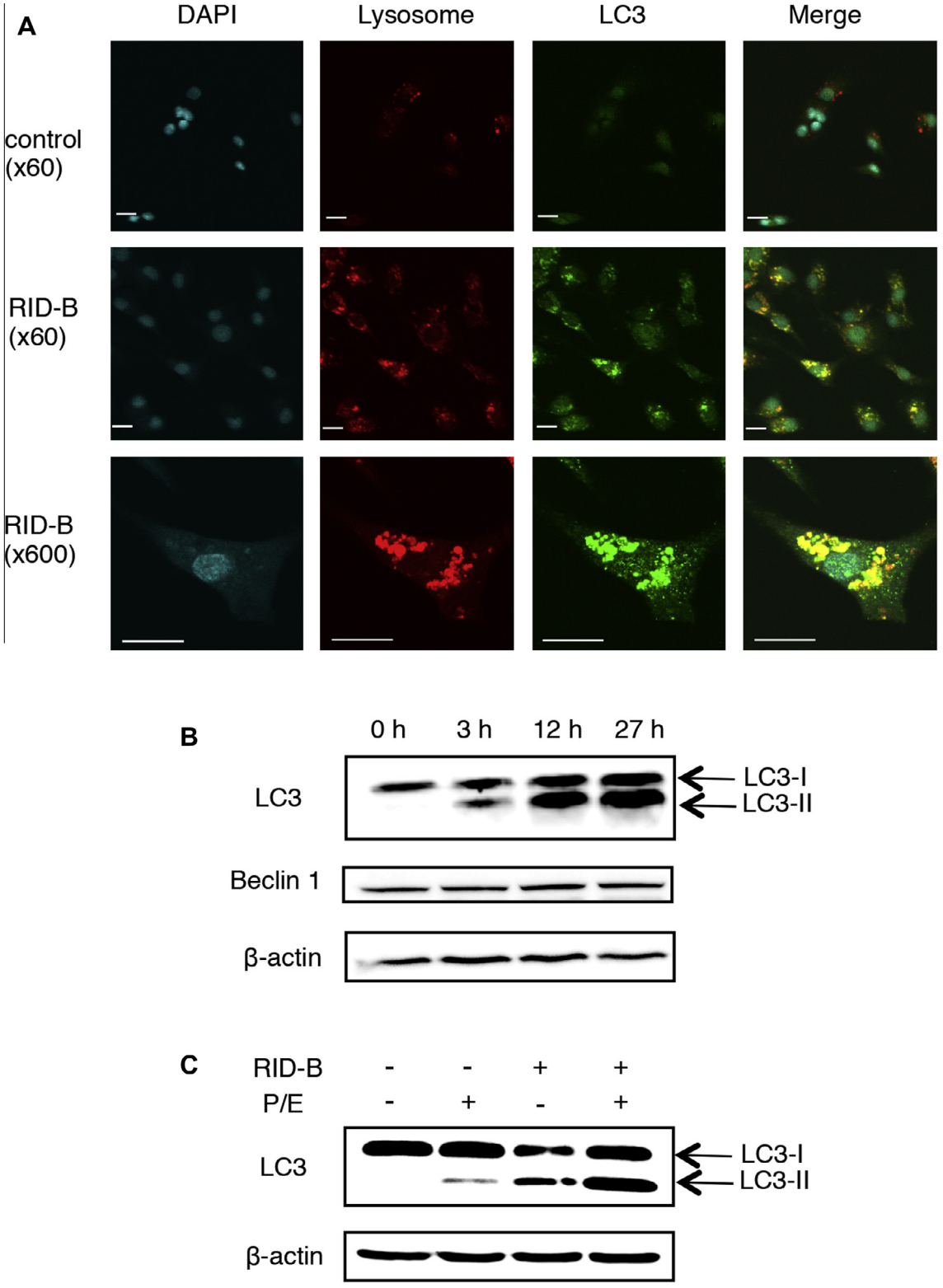

Fig. 2. RID-B induced the formation of autolysosomes and conversion of LC3. (A) HepG2 cells were incubated with 0.5 μM RID-B for 27 h. Cells were labeled with fluorescence and imaged by confocal microscopy. Red, Lysotracker Red-labeled lysosomes; green, Alexa Fluor 488-labeled LC3; blue, DAPI-labeled nucleus. The orange-stained cells indicated LC3 colocated with lysosomes. White bar indicates 20 μm. (B) Jurkat cells were incubated with 0.4 μM RID-B for the indicated times. The switch of LC3-I to LC3-II, Beclin-1 and β-actin were detected by Western blotting. β-Actin was detected as equal protein loading. (C) Jurkat cells were incubated with 0.4 μM RID-B and/or 10 μg/mL pepstatin A with 10 μg/mL E-64-d (P/E) for 24 h. The switch of LC3-I to LC3-II and β-actin were detected by Western blotting. β-Actin was detected as equal protein loading. (For interpretation of color in this figure, the reader is referred to the web version of this article.)

olysis and lipidation [20,21]. Since Jurkat cells are suspension cells, they are difficult to observe, and thus we used HepG2 cells in this assay. Lysosomes were stained with a specific dye (Lysotracker Red) to visualize the colocalization of LC3. In the nonadditive control cells, little LC3 localization was observed, and lysosomes were indistinctly stained. However, treatment with 0.5 μM RID-B for

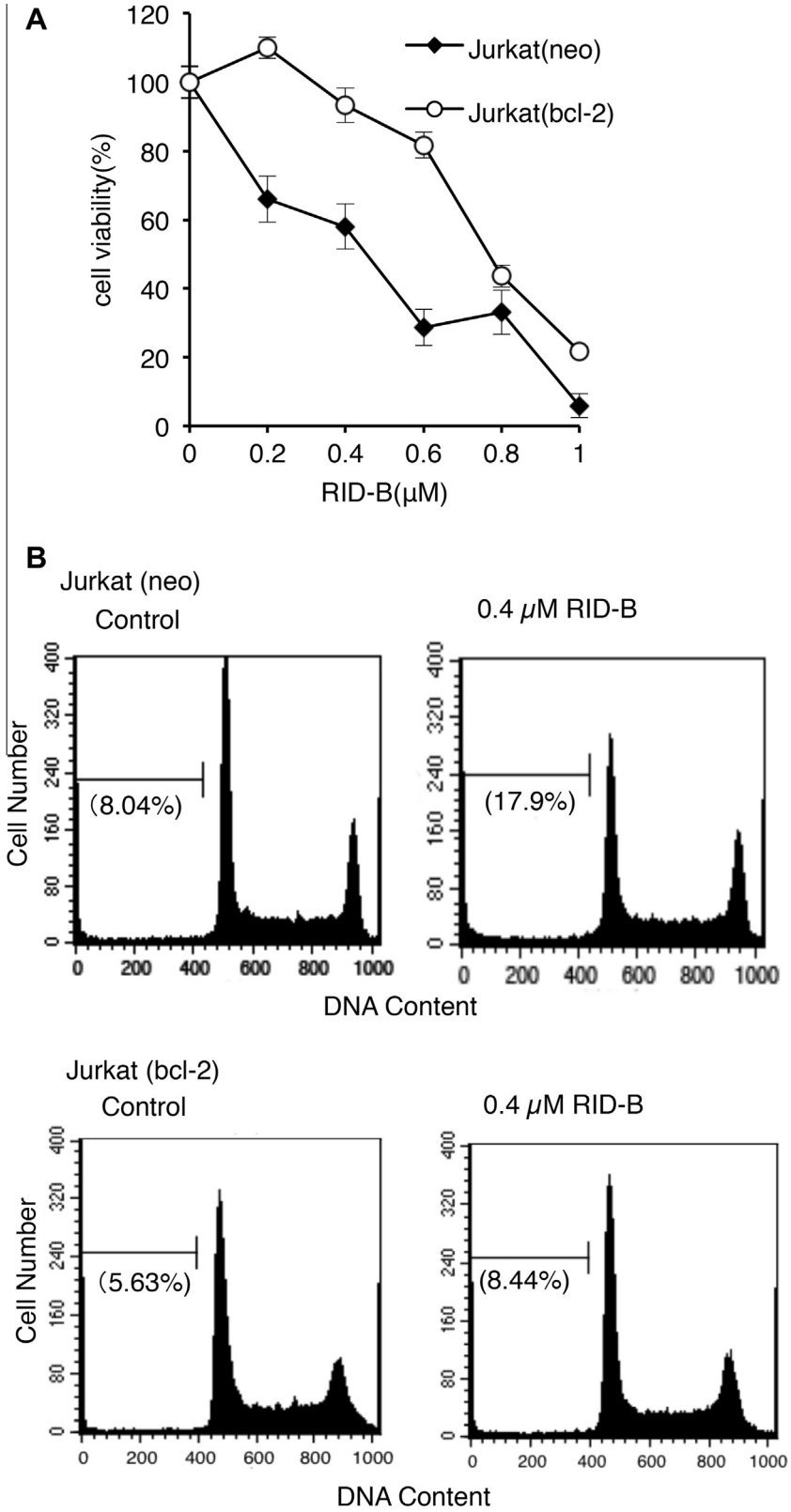

Fig. 3. Overexpression of Bcl-2 blocked RID-B-induced apoptosis. (A) Jurkat (neo) and Jurkat (Bcl-2) cells were incubated with the indicated doses of RID-B for 24 h. Cell viability was observed with an MTT assay. The results are presented as a comparison to the nonadditive control. Each bar = std. dev. ($n = 3$). (B) Jurkat (Bcl-2) cells were incubated with 0.4 μM RID-B for 24 h and assayed flow cytometrically as described in Section 2. Data are representative of three independent experiments. Parentheses indicate the percentages of sub-G1 phase.

27 h resulted in huge lysosomes, and LC3 was colocalized with lysosomes, demonstrating the formation of autolysosomes (Fig. 2A).

Moreover, the conversion of LC3-I into LC3-II during autophagy was observed. We determined the LC3 conversion of LC3-I to LC3-II in Jurkat cells by Western blotting. An attenuation of LC3-I and in-

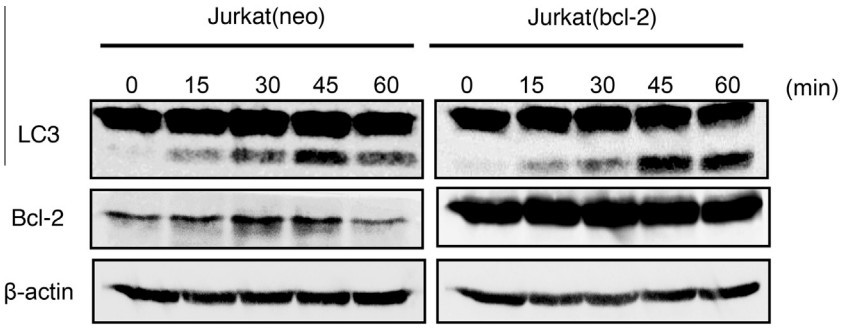

Fig. 4. Overexpression of Bcl-2 did not inhibit RID-B-induced autophagy. Jurkat (neo) and Jurkat (Bcl-2) cells were incubated with 0.4 μM RID-B for the indicated times. The switch of LC3-I to LC3-II was detected by Western blotting. β-Actin was detected as equal protein loading.

crease of LC3-II in a time-dependent manner was observed (Fig. 2B). We also estimated autophagic flux, which is important to distinguish increased autophagosome formation from impaired degradation. Addition of protease inhibitors pepstatin A/E-64-d for blocking lysosome activity further increased RID-B induced LC3-II protein level (Fig. 2C), indicating that autophagy was induced by the RID-B treatment (Fig. 2B).

We also identified another autophagy-related protein. During conventional autophagy, Beclin 1 contributes to progress autolysosome conformation [5]. Here, RID-B treatment did not increase the Beclin 1 level, suggesting that Beclin 1 is not involved in RID-B-induced autophagy (Fig. 2B).

3.3. RID-B-induced autophagy is independent of Bcl-2

In our previous study, we revealed that overexpression of the mitochondria-localized anti-apoptotic protein Bcl-2 in Jurkat cells overcame RID-B-induced apoptosis at 4 μM in a short period of time, 4 h [17]. As shown in Fig. 3A, the overexpression of Bcl-2 clearly inhibited the RID-B-induced decrease in cell viability even after long-term treatment (24 h). At doses of 0.4 μM, the viability of Jurkat cells dropped to 60%, since Bcl-2-overexpressed cells were not damaged at all. Moreover, the overexpression of Bcl-2 blocked the RID-B-induced fragmentation of DNA (Fig. 3B), indicating that Bcl-2 overexpression certainly inhibited RID-B-induced apoptosis.

Bcl-2 binds to Beclin 1 and inhibits conventional autophagy pathway [9,10]. We therefore determined whether Bcl-2 overexpression inhibits RID-B-induced autophagy. As shown in Fig. 4, Bcl-2 overexpression did not alter RID-B-induced LC3-II conversion compared to the control cell line. This result confirms that RID-B-induced autophagy is independent of Beclin 1, and that the RID-B-induced autophagy pathway is different from the conventional autophagy pathway.

4. Discussion

In this study, we treated ER-negative Jurkat cells with the novel tamoxifen derivative RID-B and observed RID-B-induced autophagy at a very low RID-B dose (0.4 μM). During RID-B-induced autophagy, the Beclin 1 level was unchanged. Moreover, overexpression of the mitochondria-localized anti-apoptotic protein Bcl-2 suppressed RID-B-induced cell death, but not autophagy. These results suggested that mitochondria perturbation, which is a main factor in RID-B-induced apoptosis, is not involved in RID-B-induced autophagy, and that RID-B-induced autophagy is different from the conventional autophagy pathway.

In our recent study, we discovered that sub-micromolar doses of RID-B could quickly induce apoptosis despite ER expression. In the present study, low-dose (0.4–0.5 μM) RID-B was administered to ER-negative cells (Jurkat) and ER-positive cells (HepG2), and both cell lines then showed typical LC3 conversion, suggesting that RID-B-induced autophagy is ER-independent, similar to RID-B-induced apoptosis. The original compound tamoxifen also induces autophagy. Schoenlein et al. and others reported that tamoxifen induced autophagy in ER alpha cells [22], but there are no such reports with ER-negative cells, to our knowledge. In the present study, the tamoxifen derivative RID-B induced autophagy despite an ER defect.

Poirot et al. reported that tamoxifen accumulates free sterol and leads to autophagy [23]. In the case of Niemann–Pick disease, cholesterol accumulation resulted in autophagy [24]. Similarly, we found that RID-B accumulated free sterol in HepG2 cells (data not shown). Further studies are needed to determine the involvement of sterol accumulation in RID-B-induced autophagy, and they may clarify the ER independence of the RID-B-induced autophagy pathway.

In our previous study, RID-B-induced apoptosis was mediated by mitochondria perturbation [17]. Bcl-2 overexpression inhibited RID-B-induced apoptosis phenomena including a mitochondria membrane potential decrease, caspase activation and DNA fragmentation. However, Bcl-2 overexpression did not overcome RID-B-induced autophagy. These results suggest that mitochondria perturbation, which is a main factor in RID-B-induced apoptosis, is not involved in RID-B-induced autophagy.

Autophagy signaling machinery is related mainly to the inhibition of the mTOR pathway, which regulates cell growth and cell proliferation [8]. Inhibition of mTOR induced Beclin 1 upregulation, stimulating conventional autophagy process [25]. Moreover, Bcl-2 binds to Beclin 1 and inhibits this conventional autophagy pathway independent of its anti-apoptotic role [9,10]. In the present study, RID-B did not alter the Beclin 1 level at all (Fig. 2). In addition, Bcl-2 overexpression did not inhibit LC3-II conversion. These results suggest that RID-B-induced autophagy is not related to the conventional autophagy pathway, which is independent of Beclin 1.

The so-called noncanonical autophagy pathway forms autophagosomes independent of Beclin 1 and Vps34, involving LC3 [26]. Moreover, the noncanonical autophagy pathway cannot be inhibited by the PI3 K inhibitor 3-methyladenine. We have observed that RID-B-induced LC3 conversion was not inhibited by 3-methyladenine (data not shown). In light of the above findings, the RID-B-induced autophagy pathway seems to be noncanonical, which is independent of Bcl-2 and Beclin 1. Other drugs have induced similar autophagy pathways (Beclin 1-independent) [27,28].

We have observed that RID-B-induced autophagy can occur in various types of cancer cells, without dependency on ER and Bcl-2 levels. Further studies should be conducted to determine the mechanisms underlying RID-B-induced autophagy, to clarify

whether RID-B will be a clinically useful, ER-independent chemotherapeutic agent for cancer.

Acknowledgments

This study was supported by a Health and Labour Sciences Research Grants from the Ministry of Health, Labour and Welfare, Japan. We are thankful of Mr. Takashi Takashima and Mr. Atsushi Takano for technical assistance.

References

[1] N. Mizushima, Autophagy: process and function, Genes Dev. 21 (2007) 2861–2873.
[2] T. Shintani, D.J. Klionsky, Autophagy in health and disease: a double-edged sword, Science 306 (2004) 990–995.
[3] A.M. Cuervo, Autophagy: in sickness and in health, Trends Cell Biol. 14 (2004) 70–77.
[4] D. Mijaljica, M. Prescott, D.J. Klionsky, R.J. Devenish, Autophagy and vacuole homeostasis: a case for self-degradation?, Autophagy 3 (2007) 417–421
[5] S.F. Funderburk, Q.J. Wang, Z. Yue, The Beclin 1-VPS34 complex–at the crossroads of autophagy and beyond, Trends Cell Biol. 20 (2010) 355–362.
[6] S. Pankiv, T.H. Clausen, T. Lamark, A. Brech, J.A. Bruun, H. Outzen, A. Overvatn, G. Bjorkoy, T. Johansen, P62/SQSTM1 binds directly to Atg8/LC3 to facilitate degradation of ubiquitinated protein aggregates by autophagy, J. Biol. Chem. 282 (2007) 24131–24145.
[7] S. Pattingre, L. Espert, M. Biard-Piechaczyk, P. Codogno, Regulation of macroautophagy by mTOR and Beclin 1 complexes, Biochimie 90 (2008) 313–323.
[8] T. Yorimitsu, D.J. Klionsky, Eating the endoplasmic reticulum: quality control by autophagy, Trends Cell Biol. 17 (2007) 279–285.
[9] S. Pattingre, A. Tassa, X. Qu, R. Garuti, X.H. Liang, N. Mizushima, M. Packer, M.D. Schneider, B. Levine, Bcl-2 antiapoptotic proteins inhibit Beclin 1-dependent autophagy, Cell 122 (2005) 927–939.
[10] S. Oh, E. Xiaofei, D. Ni, S.D. Pirooz, J.Y. Lee, D. Lee, Z. Zhao, S. Lee, H. Lee, B. Ku, T. Kowalik, S.E. Martin, B.H. Oh, J.U. Jung, C. Liang, Downregulation of autophagy by Bcl-2 promotes MCF7 breast cancer cell growth independent of its inhibition of apoptosis, Cell Death Differ. 18 (2011) 452–464.
[11] A.C. Kimmelman, The dynamic nature of autophagy in cancer, Genes Dev. 25 (2011) 1999–2010.
[12] A. Notte, L. Leclere, C. Michiels, Autophagy as a mediator of chemotherapy-induced cell death in cancer, Biochem. Pharmacol. 82 (2011) 427–434.
[13] G. Xi, X. Hu, B. Wu, H. Jiang, C.Y. Young, Y. Pang, H. Yuan, Autophagy inhibition promotes paclitaxel-induced apoptosis in cancer cells, Cancer Lett. 307 (2011) 141–148.
[14] Y.K. Jo, S.J. Park, J.H. Shin, Y. Kim, J.J. Hwang, D.H. Cho, J.C. Kim, ARP101, a selective MMP-2 inhibitor, induces autophagy-associated cell death in cancer cells, Biochem. Biophys. Res. Commun. 404 (2011) 1039–1043.
[15] P. de Medina, S. Silvente-Poirot, M. Poirot, Tamoxifen and AEBS ligands induced apoptosis and autophagy in breast cancer cells through the stimulation of sterol accumulation, Autophagy 5 (2009) 1066–1067.
[16] K.S. Cho, Y.H. Yoon, J.A. Choi, S.J. Lee, J.Y. Koh, Induction of autophagy and cell death by tamoxifen in cultured retinal pigment epithelial and photoreceptor cells, Invest. Ophthalmol. Vis. Sci. 53 (2012) 5344–5353.
[17] Y. Nagahara, I. Shiina, K. Nakata, A. Sasaki, T. Miyamoto, M. Ikekita, Induction of mitochondria-involved apoptosis in estrogen receptor-negative cells by a novel tamoxifen derivative, ridaifen-B, Cancer Sci. 99 (2008) 608–614.
[18] I. Shiina, Y. Sano, K. Nakata, M. Suzuki, T. Yokoyama, A. Sasaki, T. Orikasa, T. Miyamoto, M. Ikekita, Y. Nagahara, Y. Hasome, An expeditious synthesis of tamoxifen, a representative SERM (selective estrogen receptor modulator), via the three-component coupling reaction among aromatic aldehyde, cinnamyltrimethylsilane, and beta-chlorophenetole, Bioorg. Med. Chem. 15 (2007) 7599–7617.
[19] I. Shiina, Y. Sano, K. Nakata, T. Kikuchi, A. Sasaki, M. Ikekita, Y. Nagahara, Y. Hasome, T. Yamori, K. Yamazaki, Synthesis and pharmacological evaluation of the novel pseudo-symmetrical tamoxifen derivatives as anti-tumor agents, Biochem. Pharmacol. 75 (2008) 1014–1026.
[20] H.E. Polson, J. de Lartigue, D.J. Rigden, M. Reedijk, S. Urbe, M.J. Clague, S.A. Tooze, Mammalian Atg18 (WIPI2) localizes to omegasome-anchored phagophores and positively regulates LC3 lipidation, Autophagy (6) (2010).
[21] Y. Kabeya, N. Mizushima, T. Ueno, A. Yamamoto, T. Kirisako, T. Noda, E. Kominami, Y. Ohsumi, T. Yoshimori, LC3, a mammalian homologue of yeast Apg8p, is localized in autophagosome membranes after processing, EMBO J. 19 (2000) 5720–5728.
[22] P.V. Schoenlein, S. Periyasamy-Thandavan, J.S. Samaddar, W.H. Jackson, J.T. Barrett, Autophagy facilitates the progression of ERalpha-positive breast cancer cells to antiestrogen resistance, Autophagy 5 (2009) 400–403.
[23] M. Poirot, S. Silvente-Poirot, R.R. Weichselbaum, Cholesterol metabolism and resistance to tamoxifen, Curr. Opin. Pharmacol. 12 (2012) 683–689.
[24] S. Ishibashi, T. Yamazaki, K. Okamoto, Association of autophagy with cholesterol-accumulated compartments in Niemann–Pick disease type C cells, J. Clin. Neurosci. 16 (2009) 954–959.
[25] S. Carloni, S. Girelli, C. Scopa, G. Buonocore, M. Longini, W. Balduini, Activation of autophagy and Akt/CREB signaling play an equivalent role in the neuroprotective effect of rapamycin in neonatal hypoxia-ischemia, Autophagy 6 (2010) 366–377.
[26] K. Juenemann, E.A. Reits, Alternative macroautophagic pathways, Int. J. Cell. Biol. 2012 (2012) 189794.
[27] F. Scarlatti, R. Maffei, I. Beau, P. Codogno, R. Ghidoni, Role of non-canonical Beclin 1-independent autophagy in cell death induced by resveratrol in human breast cancer cells, Cell Death Differ. 15 (2008) 1318–1329.
[28] D.M. Smith, S. Patel, F. Raffoul, E. Haller, G.B. Mills, M. Nanjundan, Arsenic trioxide induces a beclin-1-independent autophagic pathway via modulation of SnoN/SkiL expression in ovarian carcinoma cells, Cell Death Differ. 17 (2010) 1867–1881.